

Biomimicking Natural Wood to Fabricate Isotropically Super-strong,
Tough, and Transparent Hydrogels for Strain Sensor and Triboelectric
Nanogenerators Applications

Yitong Xie^{a,b,c}, Xiaoyu Shi^a, Shishuai Gao^a, Chenhuan Lai^c, Chuanwei Lu^c, Yuxiang

*Huang^e, Daihui Zhang^{*a,b,c}, Shuangxi Nie^{*d}, Feng Xu^{*b}, Fuxiang Chu^{a,c}*

a. Institute of Chemical Industry of Forest Products, Chinese Academy of Forestry (CAF), Jiangsu Province, No 16, Suojin Wucun, Nanjing 210042, China.

b. College of Materials Science and Technology, Beijing Forestry University, Beijing 100083, China

c. Jiangsu Co-Innovation Center of Efficient Processing and Utilization of Forest Resources, Nanjing Forestry University, Nanjing 210037, China.

d. School of Light Industry and Food Engineering, Guangxi University, Nanning 530004, China.

^e Research Institute of Wood Industry, Chinese Academy of Forestry (CAF), Beijing 100091, China.

1.1 Materials

Poplar boards were purchased from Jiashan Zhonghui Wood Industry Co., Ltd. (Zhejiang, China). Potassium hydroxide, sodium chlorite, and acetic acid were obtained from Sinopharm Chemical Reagent Co., Ltd. (Shanghai, China). Ethanol was obtained from Nanjing Chemical Reagent Co., Ltd. (Nanjing, China). [Emim]OAc (>99.0%) was bought from Lanzhou Institute of Chemical Physics, Chinese Academy of Sciences. Acrylamide (AM), *N,N'*-methylene-bisacrylamide, and 2-hydroxy-40-(2-hydroxyethoxy)-2-methylpropiophenone (Irgacure 2959) were purchased from Aladdin Chemical Reagent Co., Ltd. (Shanghai, China). Copper ethylenediamine was obtained from Macklin Chemical Reagent Co., Ltd. (Shanghai, China). All reagents were used as received without further purification.

1.2 Characterization

FT-IR spectra were recorded in the spectral range of 4000 to 500 cm^{-1} using an ATR-FT-IR spectrometer (Thermo, USA). Temperature-dependent FT-IR was performed using a Lambda 950 Fourier transform spectrometer (PerkinElmer). The samples were heated from 30 to 80 $^{\circ}\text{C}$ at a rate of 10 $^{\circ}\text{C min}^{-1}$. The viscoelastic properties of BES were analyzed by Haake Mars 60 geometry with parallel plates (20 mm in diameter) at 30 $^{\circ}\text{C}$. The storage (G') and loss (G'') moduli of the samples were recorded with an oscillation mode at a fixed oscillatory strain (γ) of 1% in the frequency range from 0.01 to 100 Hz. The morphology of the BES was observed using a cryo-SEM (SU8010, Hitachi, Japan). The morphology of the hydrogels was observed by scanning electron microscopy (SEM; Regulus 8230, Hitachi, Japan). Raman mapping and spectroscopy were performed using a Raman imaging microscope with a 532 nm wavelength (excitation laser; Thermo Scientific DXR, USA). To map the distribution of the lignin nanoparticles, Raman maps (scan range = 5 $\mu\text{m} \times 5 \mu\text{m}$, spatial resolution = 100 nm) were created using the peak height method at a peak of 708 cm^{-1} (OMNIC software). Differential scanning calorimetry (DSC; PerkinElmer Diamond, PE, USA) heating curves were collected in the range from 30 to -70°C at a cooling rate of 5 $^{\circ}\text{C min}^{-1}$. For the tensile test, the hydrogels were cut into dumbbell-shaped specimens (4 mm wide and 25 mm long). Tensile tests were performed on a universal testing machine with a 50 N load cell (Instron Co., USA) at a test speed of 100 mm min^{-1} . Measurements were conducted on at least three specimens to obtain the average values. The hydrogel modulus at a certain strain was calculated using linear fitting (stress/strain), and the

slope was defined as the modulus. The toughness was calculated from the total area under the stress–strain curve. The dissipated energy and elastic recovery were calculated as described in a previous study^[13]. The water content was calculated using the following equation:

$$\omega(H_2O) = \frac{m_s - m_d}{m_s} \times 100\% \quad (4)$$

where m_s is the weight of the hydrogel at equilibrium and m_d is the weight of the dried sample.

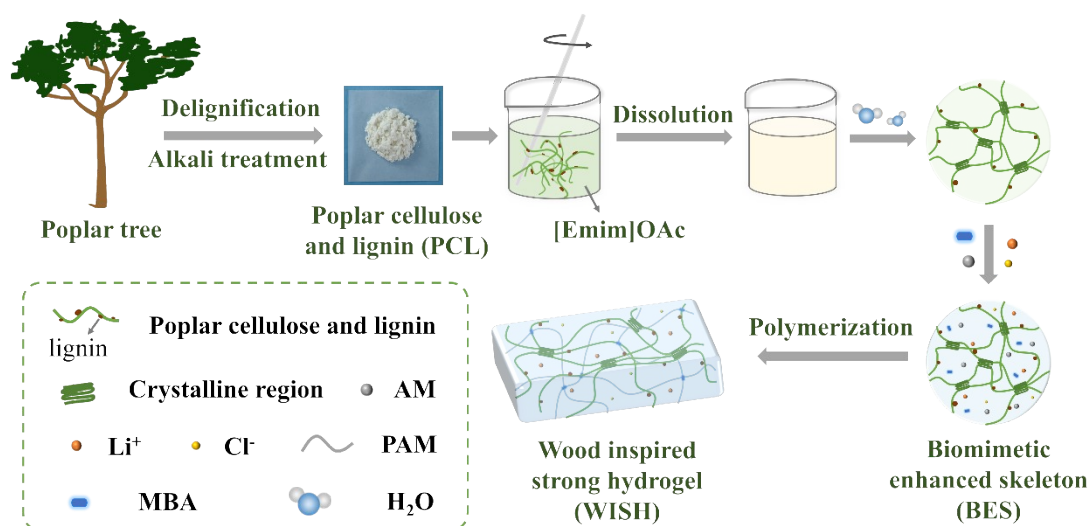


Figure S1 Fabrication process of WISH.

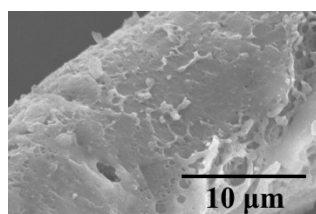


Figure S2 SEM image of poplar cellulose and lignin (PCL).

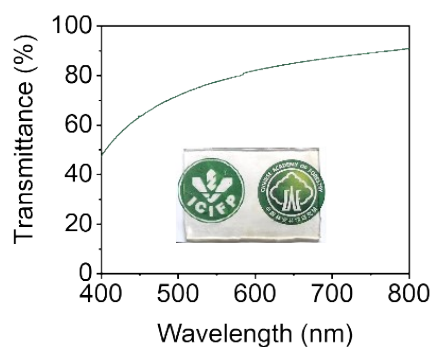


Figure S3 UV-vis transmittance spectra of WISH-7.5 at wavelength from 400 to 800 nm.



Figure S4 PCL-[Emim]OAc solution

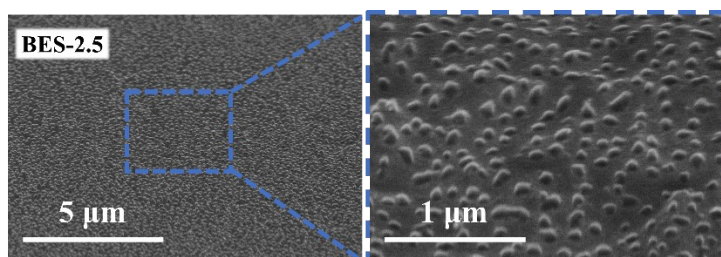


Figure S5 Cryo-SEM images of BES-2.5.

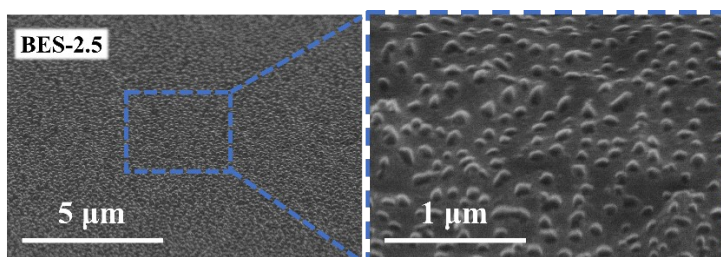


Figure S6 Cryo-SEM images of BES-5.

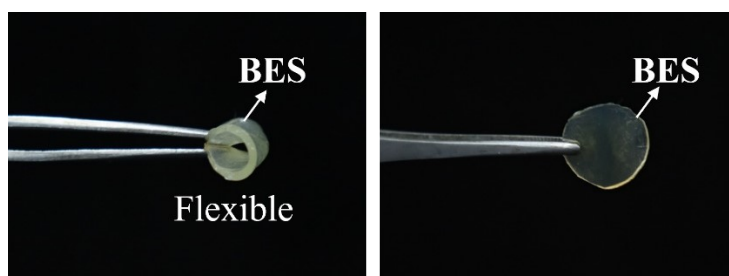


Figure S7 The photo of PCL.

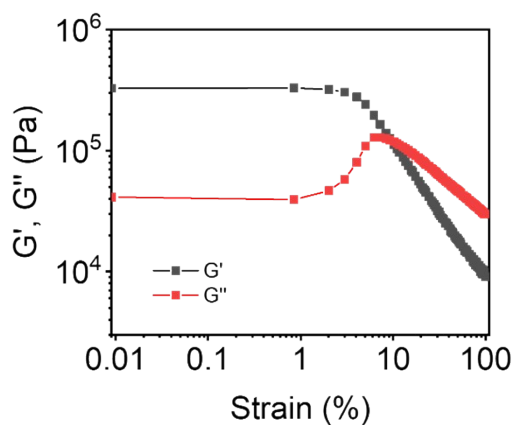


Figure S8 Complex modulus versus strain curves for BES-7.5 at the frequency of 1.00 Hz.

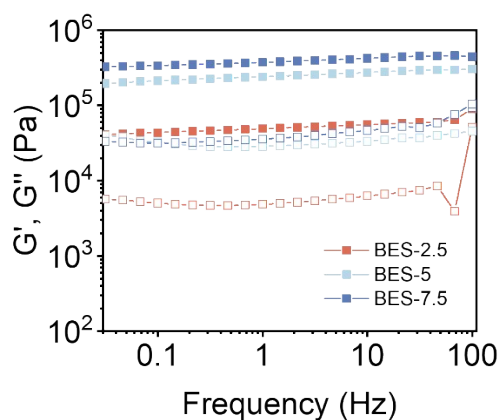


Figure S9 Storage modulus (G' , unfilled) and loss modulus (G'' , filled) of BESs at the strain of 1%.

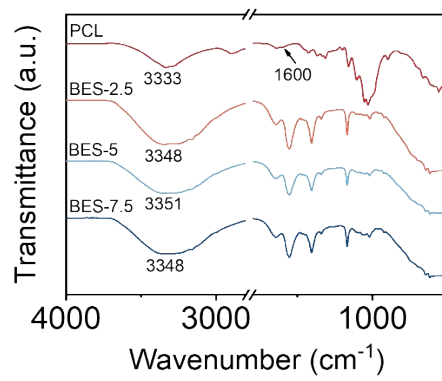


Figure S10 FT-IR spectra of PCL and BESs.

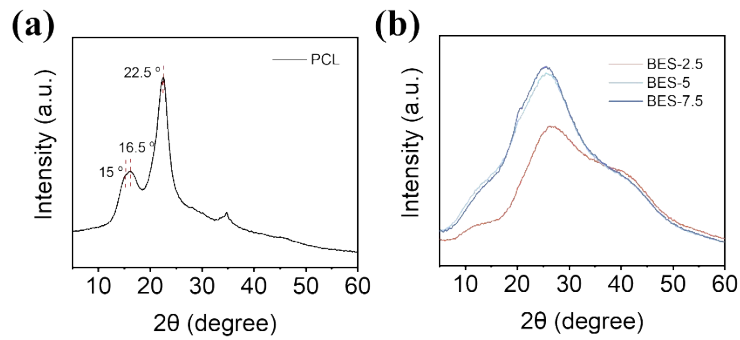


Figure S11 XRD spectroscopy of PCL (a) and BESs (b).

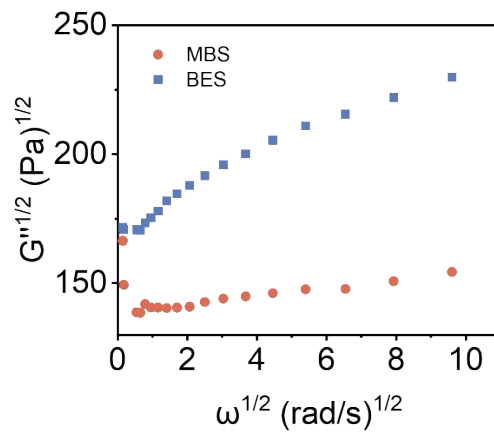


Figure S12 Casson plot for obtaining the yield stress of MBS and BES.

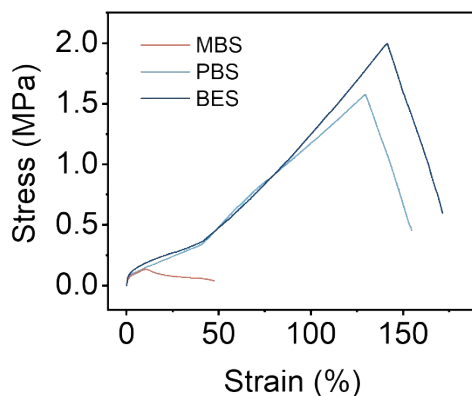


Figure S13 Tensile tests of MBS, PBS and BES.

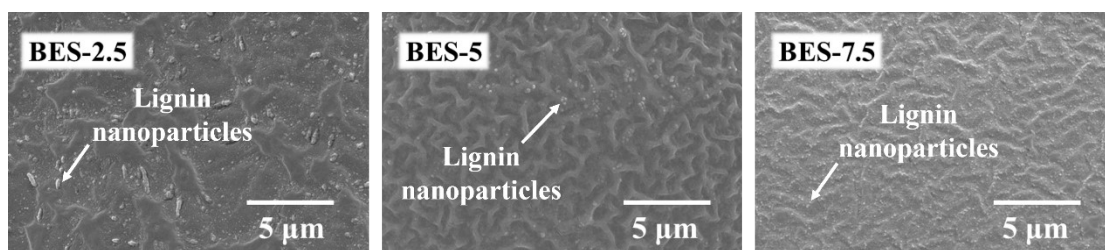


Figure S14 SEM images of BESs.

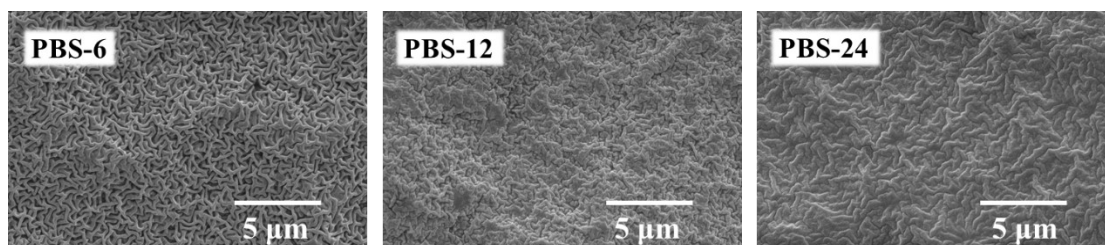


Figure S15 SEM images of PBSs.

The poplar cellulose raw materials were obtained by four-times of repeated delinification in the cellulose extraction process. The mass fraction of poplar cellulose was 7.5 wt%. The induction time of water molecules was from 6 h to 12 h, and then to 24 h, therefore, the obtain the poplar cellulose-based skeleton was noted as PBS-6, PBS-12, and PBS-24, respectively. From the SEM images, there were only dense cellulose network but no

lignin microspheres. Moreover, with the induced time increased, there are more cellulose chains reacted with ions of ionic liquid and water molecules, resulting in the denser network structure.

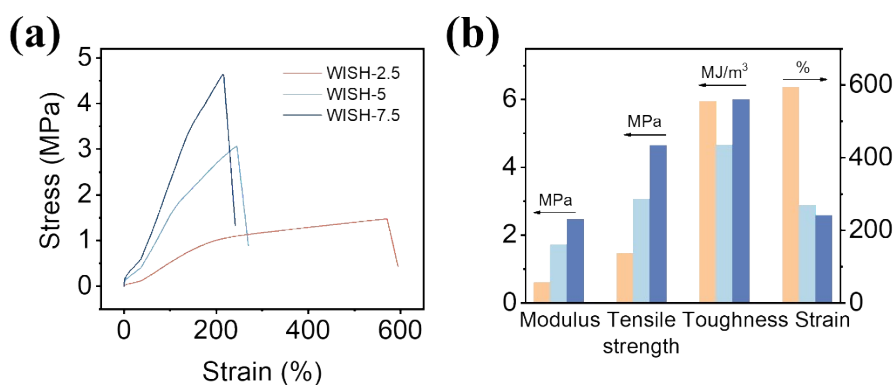


Figure S16 (a) Tensile test of WISHs; (b) calculated modulus, tensile strength, toughness, and strain of WISHs.

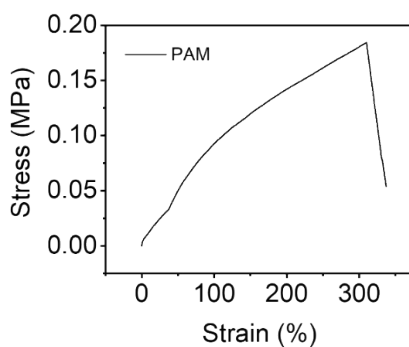


Figure S17 Tensile test of PAM.

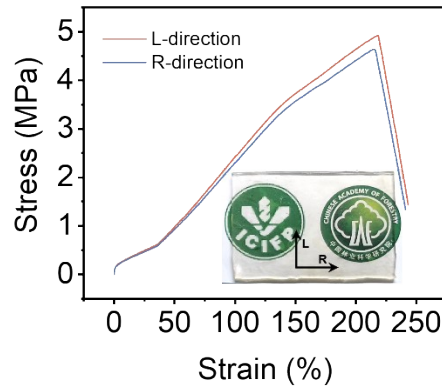


Figure S18 Tensile tests of WISH-7.5 on longitudinal and lateral directions.

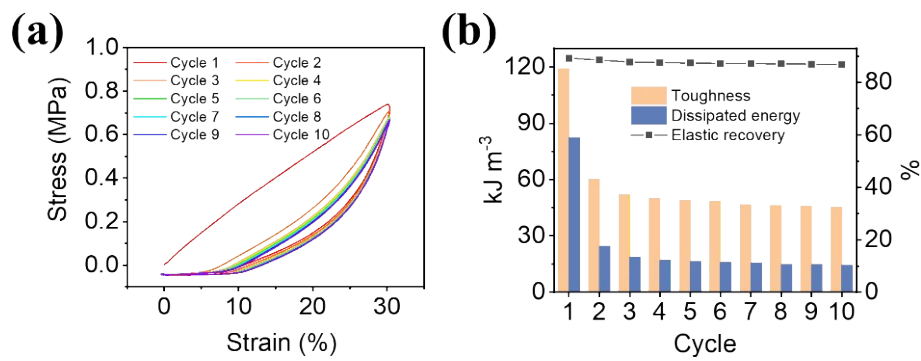


Figure S19 (a) Cyclic test of WISH-7.5 at the strain of 30 %; (b) Calculated toughness, dissipated energy and elastic recovery of WISH-7.5 from cyclic tests.

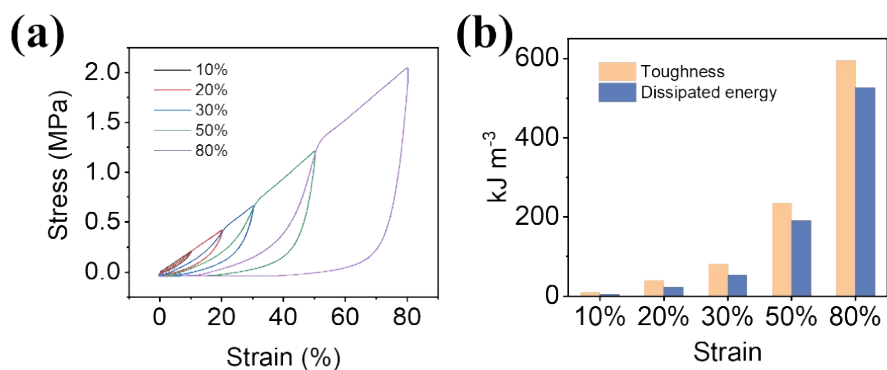


Figure S20 (a) Loading-unloading curves of WISH-7.5 with increased strain from 10 % to 80 %; (b) Calculated toughness and dissipated energy of WISH-7.5 with increased strain from 10 % to 80 %.

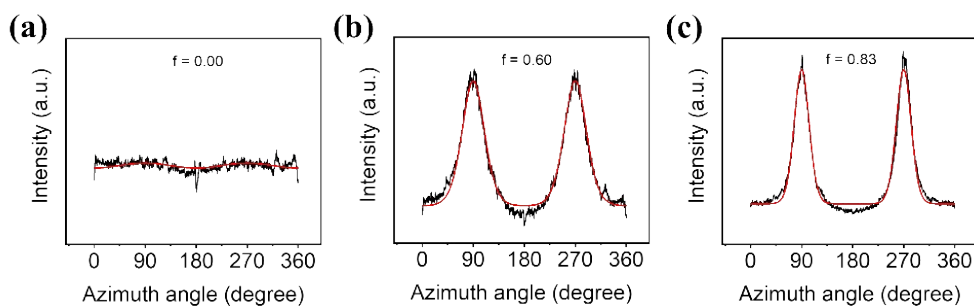


Figure S21 Typical azimuthal intensity distribution of the SAXS pattern scattering intensity obtained at a strain of (a) 0, (b) 100%, and (c) 200% for WISH-7.5. The red curve is the fitting result using the Maier-Saupe distribution function^[1].

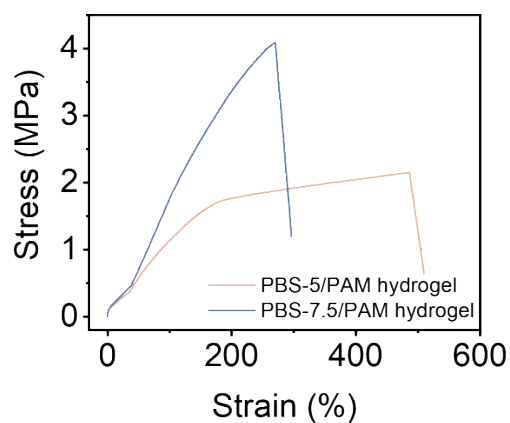


Figure S22 Tensile test of PBS/PAM hydrogels.

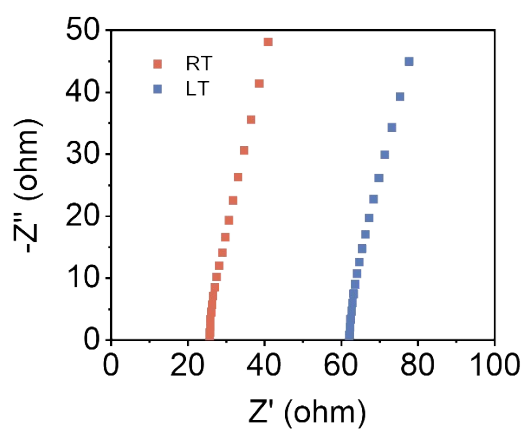


Figure S23 Electrochemical impedance spectroscopy (EIS) curves of WISH-7.5 at room temperature (25 °C) and low temperature (-29 °C).

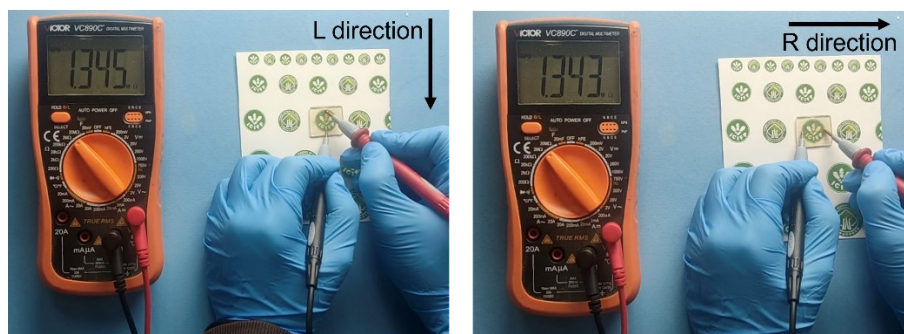


Figure S24 The resistance of WISH-7.5 on the longitudinal (L-direction) direction and lateral direction (R-direction) measured by electroprobe.

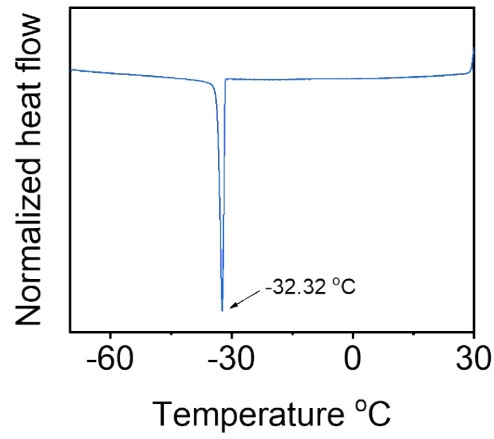


Figure S25 Differential scanning calorimetry (DSC) curve of WISH-7.5.

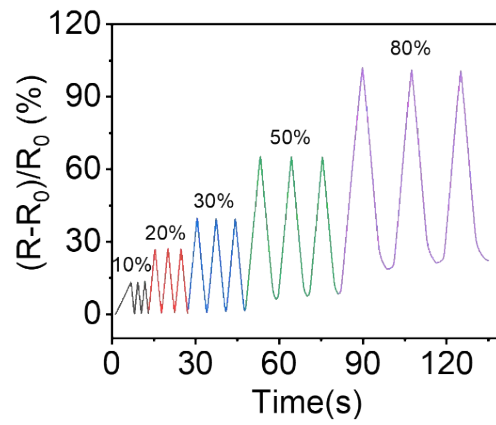


Figure S26 $\Delta R/R_0$ under the cyclic test with different strains at 10 %, 20 %, 30 %, 50 %, and 80 %

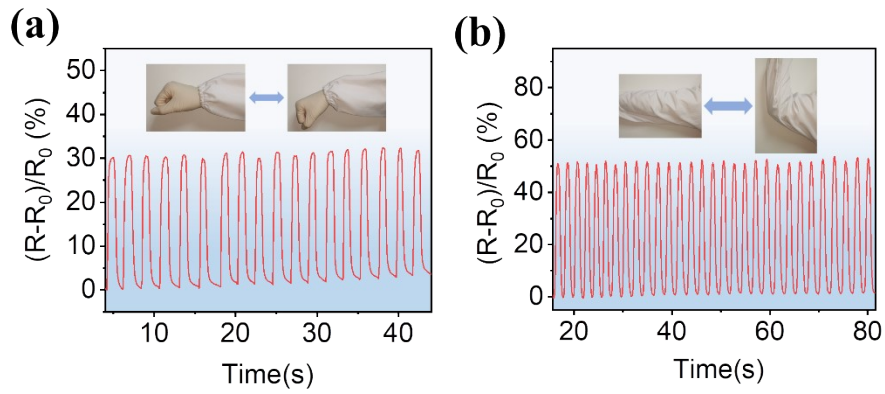


Figure S27 $\Delta R/R_0$ changes of WISH-7.5-based strain sensor versus time for real-time monitoring of repeated bending and releasing movements, wrist (a) and elbow (b).

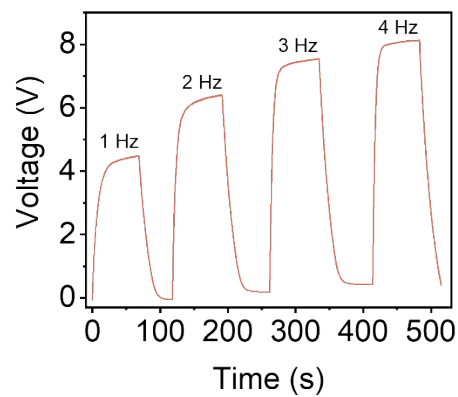


Figure S28 The charging/discharging performance of WISH-TENG for the capacitor ($2.2 \mu\text{F}$) under different pushing frequencies.

Table S1 Comparison of tensile strength of the WISH to reported hydrogels

Sample	Tensile strength (MPa)	Ref.
WISH-7.5	4.6	This work
p-Pep-Cu ²⁺	4.12 ± 0.37	[2]
Poly (MAA-co-OEGMA)	3.7	[3]
Ion-CB hydrogel	0.76	[4]
PVA-PAAm	2.5	[5]
ACA-PEG2000-ACA hydrogel	~2.9	[6]
PVA/PAM/NaCl hydrogel	0.477	[7]
Cel-IL-32 gel	3.5	[8]
DCCG composite hydrogels	2.8	[9]

Table S2 The content of chemical components

Sample	Glucan	Lignin	Xylan
Poplar raw material	47.59 %	25.37 %	17.23 %
Poplar cellulose and lignin	89.02 %	6.79 %	0.09 %

Table S3 The degree of polymerization of poplar cellulose

Parameter	Value
t	101.54
t ₀	341.83
η	3.3665
C ₀ (g/ml)	0.0051
[η] (DL/g)	3.03

Table S4 Comparison of WISH with previous strategy of fabricate

cellulose enhanced hydrogels

Sample	Type of cellulose	Toughness (MJ/m ³)	Stress (MPa)	Ref.
WISH-7.5	Poplar cellulose and lignin (PCL)	6	4.63	This work
CBH	MCC	4.3	0.8	[10]
ACH	Cotton linter pulp cellulose	1.12	1.08	[11]
Wood hydrogel	CNF	~1.08 ~2.7	0.5 36	[12]
BC-PVA-PAMPS	BC	~1.75	20.6	[13]
BC hydrogel	BC	0.14	0.68	[14]
PAM/CMC	CMC	1.0±0.05	0.1±0.02	[15]
PANa-cellulose hydrogel	Cellulose	~3.5	~0.6	[16]
CNC-C8 DPC hydrogel	CNC	~4.02	0.3±0.008	[17]
CH	Cellulose	~0.089	0.178	[18]
HPAMF	CNF	~3	0.3	[19]

Table S5 Comparison of WISH with other hydrogels

Composition	Conductivity (mS/cm)	Stress (MPa)	Toughness (MJ/m ³)	Anti-freezing	Biobased	Ref.
WISH-7.5	8.2	4.6	6.0	Yes	Yes	This work
Gelatin/Na ₃ Cit/glycerol	4.63	1.9	4.99	Yes	Yes	[20]
PHEA/SA-Ca ²⁺ /KCl	0.8	0.2	~0.4	Yes	Yes	[21]
PMZn-GL	0.56	0.875	1.05	Yes	No	[22]
PGA gel	0.34	0.28	~0.66	Yes	Yes	[23]
CH	0.036	0.178	~0.089	No	Yes	[18]

Reference

- [1] S. Feng, X. Xiong, G. Zhang, N. Xia, Y. Chen, W. Wang, *Macromolecules* **2009**, 42, 281.
- [2] B. Xue, Z. Bashir, Y. Guo, W. Yu, W. Sun, Y. Li, Y. Zhang, M. Qin, W. Wang, Y. Cao, *Nature communications* **2023**, 14, 2583.
- [3] Z. Jiang, M. L. Tan, M. Taheri, Q. Yan, T. Tsuzuki, M. G. Gardiner, B. Diggle, L. A. Connal, *Angew Chem Int Ed Engl* **2020**, 59, 7049.
- [4] S. Wang, L. Yu, S. Wang, L. Zhang, L. Chen, X. Xu, Z. Song, H. Liu, C. Chen, *Nature communications* **2022**, 13, 3408.
- [5] J. Li, Z. Suo, J. J. Vlassak, *Journal of materials chemistry. B* **2014**, 2, 6708.
- [6] S. Wang, Y. Chen, Y. Sun, Y. Qin, H. Zhang, X. Yu, Y. Liu, *Communications Materials* **2022**, 3.
- [7] G. Chen, J. Huang, J. Gu, S. Peng, X. Xiang, K. Chen, X. Yang, L. Guan, X. Jiang, L. Hou, *Journal of Materials Chemistry A* **2020**, 8, 6776.
- [8] D. Zhao, Y. Zhu, W. Cheng, G. Xu, Q. Wang, S. Liu, J. Li, C. Chen, H. Yu, L. Hu, *Matter* **2020**, 2, 390.
- [9] P. Wei, L. Wang, F. Xie, J. Cai, *Chemical Engineering Journal* **2022**, 431, 133964.
- [10] D. Zhang, J. Jian, Y. Xie, S. Gao, Z. Ling, C. Lai, J. Wang, C. Wang, F. Chu, M.-J. Dumont, *Chemical Engineering Journal* **2022**, 427, 130921.
- [11] D. Ye, P. Yang, X. Lei, D. Zhang, L. Li, C. Chang, P. Sun, L. Zhang, *Chemistry of Materials* **2018**, 30, 5175.
- [12] W. Kong, C. Wang, C. Jia, Y. Kuang, G. Pastel, C. Chen, G. Chen, S. He, H. Huang, J. Zhang, S. Wang, L. Hu, *Advanced materials* **2018**, 30, e1801934.
- [13] F. Yang, J. Zhao, W. J. Koshut, J. Watt, J. C. Riboh, K. Gall, B. J. Wiley, *Advanced Functional Materials* **2020**, 30, 2003451.
- [14] S.-Q. Chen, P. Lopez-Sanchez, D. Wang, D. Mikkelsen, M. J. Gidley, *Food Hydrocolloids* **2018**, 81, 87.
- [15] Y. Cheng, X. Ren, G. Gao, L. Duan, *Carbohydr Polym* **2019**, 223, 115051.
- [16] L. Ma, S. Chen, D. Wang, Q. Yang, F. Mo, G. Liang, N. Li, H. Zhang, J. A. Zapien, C. Zhi, *Advanced Energy Materials* **2019**, 9, 1803046.
- [17] X. Liu, X. He, B. Yang, L. Lai, N. Chen, J. Hu, Q. Lu, *Advanced Functional Materials* **2021**, 31, 2008187.
- [18] R. Tong, G. Chen, J. Tian, M. He, *Polymers (Basel)* **2019**, 11.
- [19] Y. Zhang, X. Zhao, W. Yang, W. Jiang, F. Chen, Q. Fu, *Materials Research Express* **2020**, 7.
- [20] Z. Qin, X. Sun, H. Zhang, Q. Yu, X. Wang, S. He, F. Yao, J. Li, *Journal of Materials Chemistry A* **2020**, 8, 4447.
- [21] J. Song, S. Chen, L. Sun, Y. Guo, L. Zhang, S. Wang, H. Xuan, Q. Guan, Z. You, *Advanced materials* **2020**, 32, 1906994.
- [22] Y. Feng, H. Liu, W. Zhu, L. Guan, X. Yang, A. V. Zvyagin, Y. Zhao, C. Shen, B. Yang, Q. Lin, *Advanced Functional Materials* **2021**, 31.
- [23] C. Hu, Y. Zhang, X. Wang, L. Xing, L. Shi, R. Ran, *ACS Appl Mater Interfaces* **2018**, 10, 44000.